Long Term Corrosion Protection Performance and Activity of Graphene-Based Epoxy Coating Systems for Aluminium and its Alloys

M. Sharp[1*], G. Johnson[1] and W. Weaver[1]

[1]Applied Graphene Materials plc, The Wilton Centre, Redcar, Cleveland TS10 4RF, UK

*matthew.sharp@appliedgraphenematerials.com

gaven.johnson@appliedgraphenematerials.com

william.weaver@appliedgraphenematerials.com

Keywords: Graphene, coating, barrier, passivation, catalytic

Abstract

Two different graphene nanoplatelet products, graphene and reduced graphene oxide, of differing electrical conductivity, were assessed for their corrosion protection of aluminum 5005 when incorporated into a basic epoxy coating, through both electrochemical methods and more conventional and complementary prohesion testing. In the potentiodynamic data the onset of passivation is observed at ~+18 mV from the open circuit potential in some scribed graphene-containing epoxy coatings, and this is not observed for the scribed samples containing no GNPs during the same timescale. Neither is the onset of passivation observed for the GNP-containing coatings with no scribe, where the coating itself acts as a barrier and no passivation occurs. The data suggests that the graphene, dependent on degree of conductivity, is acting to increase the rate of passivation of the metal surface, acting in a catalytic manner to increase the rate of oxidation of aluminium to alumina within the scribed region. The increased passivation layer build up within the scribed region essentially acts to seal up the scribe in a self-healing type behaviour.

1. Introduction

Applied Graphene Materials UK Ltd. produces a range of dispersions of graphene nanoplatelets (GNPs), enabling property introductions/enhancements such as electrical/thermal conductivity, mechanical e.g. fracture toughness, gas permeability and barrier type to be achieved. GNPs are manufactured using the company's patented proprietary "bottom up" process, yielding high specification graphene materials.

The active constituents of inhibitive coatings are typically marginally water soluble and produce active species which inhibit the ongoing corrosion of the metallic substrate. The active constituents historically have been chromates but other species such as phosphates, molybdates, nitrates, borates and silicates are also used. The selection of active constituents is increasingly subject to regulatory pressures due to increased concerns for the environment and health and safety.

Active inhibitor pigments undergo a partial dissolution in the presence of water when the water enters the coating. At the metal substrate surface the dissolved ions react and form a

reaction product which serves to passivate the surface, providing protection from corrosion. Such active pigments must possses sufficient solubility in water to release ions for reaction, but too much solubility may result in blistering of the coating; such a balance is often hard to achieve when formulating a coating.

An ideal coating pigment should be dual action. That is to say that the pigment should offer a barrier against water and corrosion inducing ions whilst also releasing a sufficient quantity of inhibitor ions. These two requirements are antagonistic in principle and the inhibitive coating again requires a difficult balance between barrier properties and the solvation ability.

It is acknowledged that GNPs, both as prepared and chemically functionalised, when incorporated into a coating system or host matrix, provide a highly tortuous pathway which acts to impede the movement of aggressive species towards the metal surface [1], a passive corrosion protection mechanism. In support of this, previous work has demonstrated that very small additions of GNPs decreased water vapour transmission rates [2], indicating a barrier type property, while some authors also report an electrochemcial activity provided by graphene within coatings [3].

This work aims to examine both the barrier properties and any electrochemcial influence on corrosion provided by graphene within an epoxy-based coating, through both salt spray and electrochemical test methods.

2. Experimental

2.1 Material and sample preparation

Two different graphene nanoplatelet products, reduced graphene oxide (RGO) and graphene (Applied Graphene Materials UK Ltd.), were used in this study. The basic properties of these materials are listed below in Table 1. SEM micrographs of these materials are presented in Figure 1.

Product Grade	**Basic description**	**Surface area (m^2/g)**	**Oxygen content (%)**	**Resistivity (Ω.m)**
RGO	Reduced graphene oxide	50	10-20	50000
Graphene	Graphene	350	5	0.0037

Table 1: Various properties of graphene products used in this work (Applied Graphene Materials UK Ltd.)

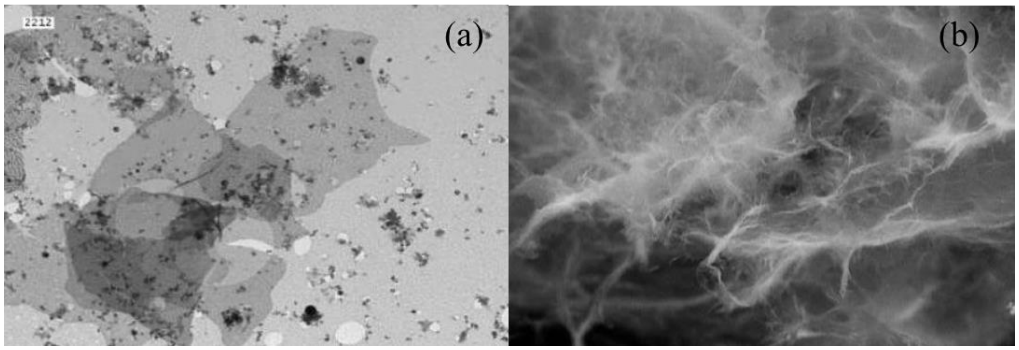

Fig.1: SEM micrographs of (a) RGO and (b) graphene nanoplatelet products

Various loadings of graphene nanoplatelets were incorporated into an epoxy resin system (BPA type epoxy and an amine-based fast hardener (5:1 mix ratio)). All coatings were resin only clears and not fully formulated products. RGO was incorporated at 0.5%, 0.03% and 0.003% by weight, while graphene was incorporated at 0.1%, 0.03% and 0.003% by weight. A graphene free epoxy coating was also evaluated alongside an uncoated (bare metal) aluminium 5005 and blasted steel substrates.

Each of the coatings were applied to aluminium (5005 grade) panels, of dimensions 150 x 100 x 2mm, by means of a conventional gravity-fed spray gun, equipped with a 1.2mm tip. Prior to coating application, the panels were degreased using acetone. The panels were allowed to cure for 1 week at ambient temperature before commencing testing. Dry film thickness of the prepared coatings were in the range of 40-60 microns.

Panels were tested in both scribed and unscribed forms (electrochemical tests only). Scribed samples were studied since they offer an immediate study of a bare metal surface in contact with electrolyte and functional coating (triple phase boundary), without having to observe the prior lengthy breakdown/degradation of the functional coating e.g. due to water uptake.

2.2 Prohesion/salt spray testing

The panels were placed in a corrosion chamber, running ASTM G85 annex 5 (prohesion) for a period of up to 4000 hours. This consists of a 1 hour cycle dry at 35°C, followed by 1 hour of salt mist spray at 23°C. Panels were assessed at 500 hour intervals for signs of blistering, corrosion, and corrosion creep in accordance with ISO4628. The assessment of the degree of corroded area was as shown in Table 2.

Degree of corrosion	**% Area**
Ri 0	0
Ri 1	0.05
Ri 2	0.5
Ri 3	1
Ri 4	8
Ri 5	40 to 50

Table 2: Degree of corrosion assessment used as part of ISO4628

2.3 Electrochemical measurements

All electrochemical measurements were recorded using a Gamry 1000E potentiostat in conjunction with a Gamry ECM8 multiplexer to permit the concurrent testing of up to 8 samples per experiment. Each individual channel was connected to a Gamry PCT-1 paint test cell, specifically designed for the electrochemical testing of coated substrate samples.

Within each paint test cell, a conventional three-electrode system, the bare aluminium, coated epoxy aluminium and scribed coated epoxy aluminium samples represented the working electrode, a graphite rod served as a counter electrode and a saturated calomel electrode (SCE) served as the reference electrode. The test area of the working electrode was 14.6 cm^2. All tests were run using a 3.5 wt.% NaCl electrolyte.

For all samples, electrochemical testing consisted of cycle of experiments comprising of electrochemical AC impedance spectroscopy (EIS) measurements and potentiodynamic polarisation scans. Since this work is focused on the change in electrochemical properties over time, each cycle of experiments was conducted at approximate intervals of 2 hours over a period of up to 1 week for all samples.

During all EIS experiments, an AC voltage of 10 mV was applied across the sample, with a zero volts DC bias, over a frequency range of 1 MHz to 0.05 Hz. Ten measurements were recorded for every decade in frequency. An integration time of 1 second per measurement was used with a delay time of 0.2 seconds between each measurement. Equivalent circuit fitting to the obtained data was performed using the proprietary Gamry Echem Analyst software package.

Potentiodynamic polarisation scans were carried out in order to generate Tafel polarisation curves. These curves were produced as a result of applying a potential of ±250 mV from the open circuit potential (500 mV sweep) at a scan rate of 0.5 mV/second with a sample period of 1 second. Data fitting to the Tafel region was carried out using the proprietary Gamry Echem Analyst software in order to extract values for the anodic and cathodic Tafel constants, E_{corr}, and corrosion rate.

3. Results & discussion

3.1 Prohesion/salt spray testing

The images shown below in Figure 2 were recorded following 4000 hours prohesion testing for all samples, including uncoated 5005 aluminum and a graphene free epoxy coating.

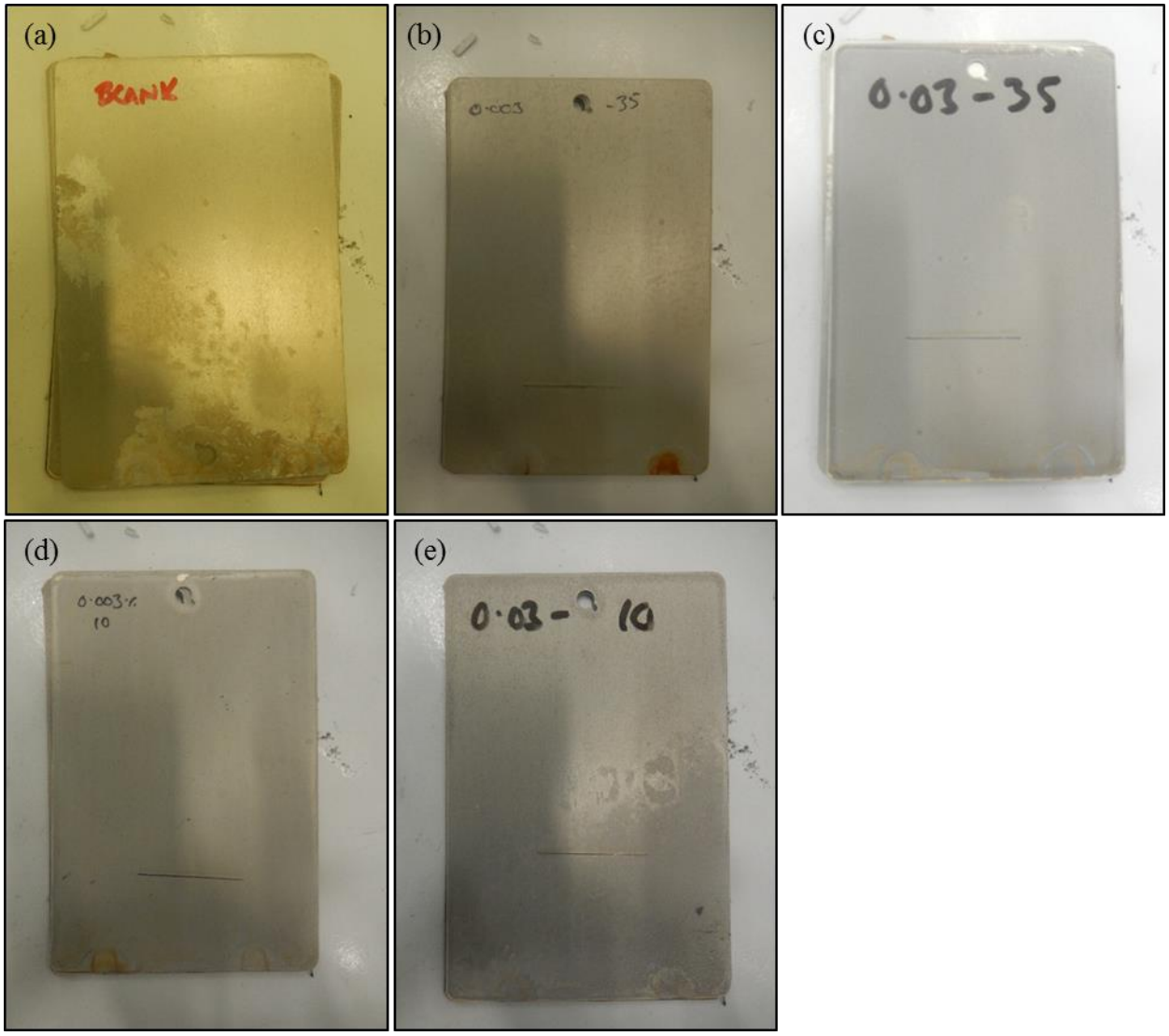

Fig. 2: Coated aluminum 5005 samples following 4000 hours prohesion testing, showing (a) blank epoxy coating and graphene-incorporated epoxy coatings of (b) 0.003 wt.% graphene, (c) 0.03 wt.% graphene, (d) 0.003 wt.% RGO and (e) 0.03 wt.% RGO

Following 4000 hours of prohesion testing, it was observed that the blank epoxy coated sample had a relatively large amount of corrosion visible on the metal surface, suggesting a majority coating failure during the prohesion test. This test panel was graded as Ri 5 for degree of corrosion (40-50 %) Some signs of coating delamination were also evident in this sample.

No obvious signs of corrosion were noted in any of the graphene-incorporated epoxy samples, across both graphene nanoplatelet types, even with graphene loadings as low as 0.003 wt.%, where a barrier type effect from the graphene nanoplatelets would be relatively low. In terms of corrosion performance, no notable difference was seen between the RGO and graphene loaded epoxy coatings.

In some cases the presence of pin holing/fisheyes are acknowledged. Such a feature with this combination of graphene type and loading may be present and is often unavoidable since the samples were not based on a fully formulated system, where, otherwise, such defects may be removed. Despite such defects, no corrosion was observed at the defect points.

No coating delamination or blistering was found on the graphene-incorporated epoxy samples.

No measurable creep was found in any of the RGO epoxy samples, where creep was observed in all of the graphene epoxy samples. This creep value was consistent across all of the different loadings of graphene and was approximately 1.2 mm during the 4000 hour duration

3.2 AC Impedance Spectroscopy (EIS)

Water uptake in organic coatings and polymers can be measured using a variety of different techniques such as the more traditional gravimetric methods [4] and capacitance methods [5]. Capacitance methods rely the creation of a capacitor over time due to water uptake in the organic coating. Water has a dielectric constant around 30 times that of most organic coatings, and the change of capacitance as water enters the coated substrate is related to the level of water uptake. Such dielectric type capacitance information can also be derived from EIS data, although there are several additional advantages of using EIS.

EIS is a non-destructive test method, applicable to a wide variety of test cases across a spectrum of different materials, both organic and inorganic [6,7]. When applied to the study of organic-based protective anticorrosive coatings, impedance values, in their straight form, provide an indication of corrosion protection. Such values may be used as an initial screening for coating barrier type performance. In addition, through the appropriate equivalent circuits modelling of EIS data, additional critical information can be obtained such as pore resistance and coating capacitance along with interfacial properties, where a coating is breached, such as double layer capacitance.

The main contribution of the coating towards impedance occurs within the lower frequency region, at a frequency close to 0.1 Hz. This feature may be used as a type of screening method in the selection of suitable organic coatings. In a review paper concerning the performance of fast-cure epoxies for pipe and tank linings, O'Donoghue et al describe the use of EIS as such a screening tool [8], where the coating impedance measured at a frequency of 0.1 Hz can be used for screening materials. O'Donoghue et al assign impedance values of 10^4 Ohm.cm^2 to poor coatings and impedance values of 10^{10} ohm.cm^2 to excellent coatings (Figure 3). Since the O'Donoghue paper, several others have also employed this screening method to measure coating performance [9, 10].

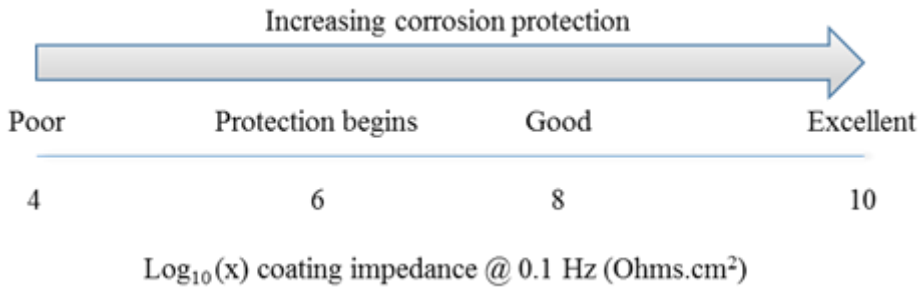

Fig.3: Corrosion protection of organic coatings. Redrawn from [8]

Figure 4 shows a selection of bode plots for both uncoated and coated metal substrates, all recorded after approximately 60 hours of testing. Although not intrinsically part of this study, a sample of bare blasted steel has also been included with the sample set as an example of a metal which does not display passivation. As would be expected, the low frequency impedance of this sample is comparatively low, between 10^2 and 10^3 Ohm.cm^2, since the corrosion products of steel are not strongly bound to the metal surface and very little protection is offered. The sample of uncoated aluminium offers a comparatively higher impedance, on the order of 10^5 Ohm.cm^2, due to the presence of the [more strongly bound] formation of a passivation layer on the metal surface, although the impedance value of this passivation layer falls in between 'poor' and 'protection begins' categories.

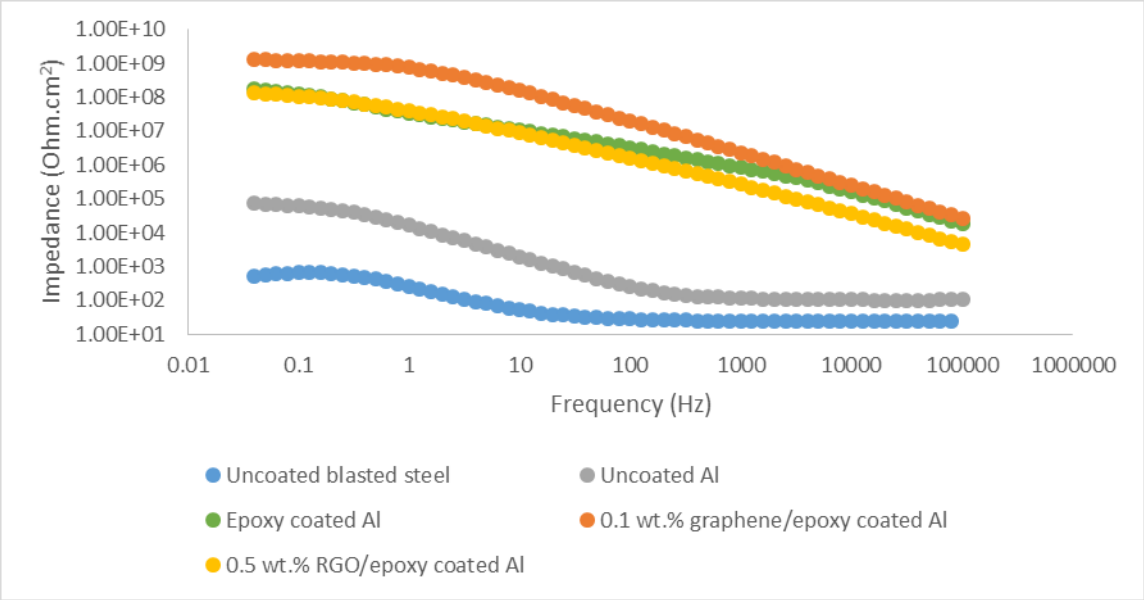

Fig.4: Bode plots showing the impedance modulus for bare steel, bare aluminium, epoxy-coated aluminium, 0.1 wt.% graphene/epoxy coated aluminium and 0.5 wt.% RGO/epoxy coated aluminium, post 60 hours immersion

The low frequency portion of the bode plot for the epoxy coated aluminium sample displays an impedance of the order of 10^8 ohm.cm^2, which places this coating firmly within the 'good' category with respect to corrosion protection. Sitting an order of magnitude above the straight epoxy sample is the 0.1 wt.% graphene in epoxy coated aluminium sample, giving a corrosion

protection between ‘good ‘and ‘excellent’. This suggests that the addition of graphene to the epoxy has led to an improvement in the coating’s barrier properties.

It is observed that the low frequency portion of the bode plot for the 0.5 wt.% RGO in epoxy coated aluminium sample displays an impedance similar to that of the epoxy coated blank at this relatively short duration.

It should be highlighted that the overall impedance of the aluminium coated samples will be made up of impedance contributions from both the natural passivation layer and the coating itself. It would be expected that, upon a breakdown of the coating, the impedance would drop back to the baseline level observed in the bare aluminium sample i.e. impedance contributions from the passivation layer only. It is recognised that coating performance is not simply concerned with high impedance values measured at low frequency, but it is also the ability of a coating to maintain such impedance values over extended periods of time. It has previously been reported that the introduction of graphene into organic coatings has led to increased sustained levels of impedance [11]. The authors of this work acknowledge that the EIS studies carried out are relatively short in length in comparison to similar studies, and, as a result, little change in the impedance measured at 0.1 Hz is observed for the experimental duration. Figure 5 shows the impedance modulus at 0.1 Hz for various coated samples over the duration of the experiment. The impedance for both the epoxy and 0.1 wt.% graphene samples in unscribed form remains fairly static throughout the experiment, reflecting the values shown in Figure 4. Figure 5 also shows the impedance of scribed versions of epoxy and 0.1 wt.% graphene samples. Since both of these coatings are effectively breached due to the scribe, a lower impedance value for both, compared with unscribed versions, would be expected. It is observed that both the epoxy and 0.1 wt.% graphene coatings give a low frequency impedance value of between 10^5 and 10^6 ohm.cm^2.

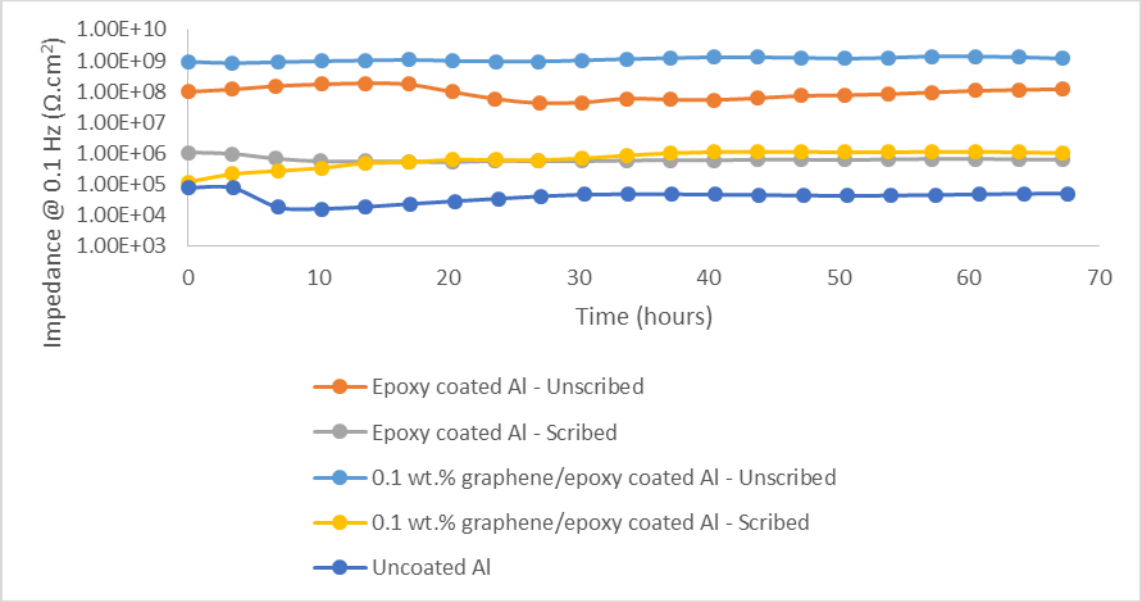

Fig.5: Change of impedance modulus at 0.1 Hz over time for coated samples

The only noticeable changes in impedance came from the uncoated aluminium samples. Figure 6 shows the low frequency impedance change for 4 uncoated aluminium samples (measured over a surface area of 14.6 cm^2). Throughout the duration of the experiment, the low frequency impedance increases slightly, due the gradual build-up of the passivation layer. It was not possible to detect a change in impedance for the scribed coated samples, presumably due to the relatively small surface area of the scribe regions.

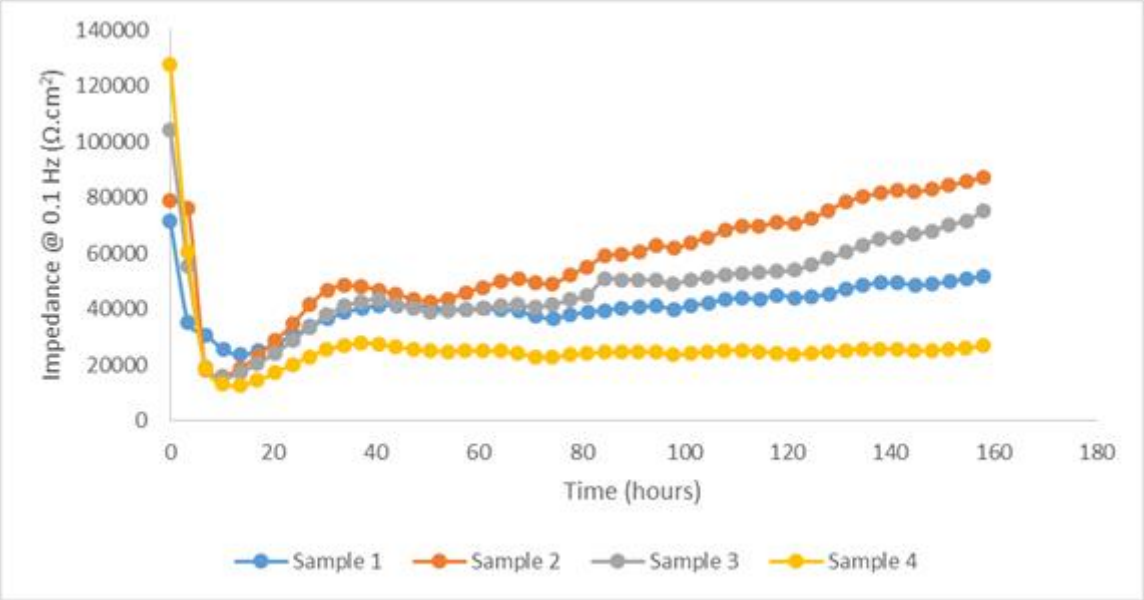

Fig.6: Change of impedance modulus at 0.1 Hz over time for uncoated aluminium samples

In order to assess the performance of these coatings over a longer duration, such EIS experiments would need to be run for longer periods, and may be subject of future work. In order to examine the immediate exposed surface area, equivalent circuit modelling was carried out on the scribed coated samples using the equivalent circuit model shown in Figure 7.

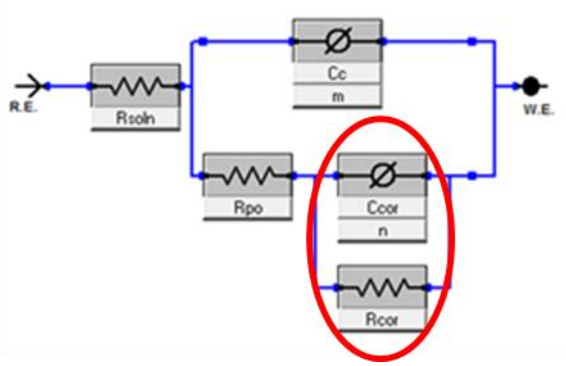

Fig.7: Equivalent circuits model used in the fitting of scribed panel data (interfacial properties highlighted)

In circumstances where an organic coating has become breached, for example through water uptake or by damage to the coating, the equivalent circuit model shown in Figure 5 may be used to model the EIS data. Through introducing a scribe into the coated sample, this intentional breaching of the coating reveals the triple phase boundary area incorporating bare metal, coating edge and electrolyte (and the model shown in Figure 5 now applies). The elements which make up this model include R_{soln} (the resistance of the electrolyte), Cc (coating capacitance), R_{po} (pore resistance), C_{cor} (double layer capacitance) and R_{cor} (corrosion resistance). The coating capacitance and pore resistance elements are properties associated with the coating itself, whereas the double layer capacitance and corrosion resistance are interfacial properties and exist when electrolyte meets the metal surface. The presence of electrolyte at the interface generates a double charge layer, which may be measured as a capacitance, with greater capacitance values indicating a larger presence of electrolyte at the interface, and greater levels of corrosion. R_{cor} is a kinetic parameter associated with the electron transfer process and is related to corrosion rate. Larger values of R_{cor} indicate a lower rate of corrosion.

Since little change was noted in the coatings properties for all samples over the course of the experiments, due to the relatively short experimental run time, attention was focused on the interfacial properties of the scribed samples. Values extracted from the circuit element values are shown in Table 3. The values of solution resistance are included since uniformity within these values provides an indication how the; values should be roughly equal since he electrolyte remains constant, although some variation may be expected if there any slight differences in electrode placement within the test cell. All solution resistance values were found to be roughly equivalent, suggesting a good fit of the impedance data to the chosen equivalent circuit model.

Circuit element	Epoxy blank	0.003 wt.% graphene	0.03 wt.% graphene	0.1 wt.% graphene	0.003 wt.% RGO	0.03 wt.% RGO	Uncoated Al
Solution resistance, R_{soln} (Ω)	22.97	23.62	17.27	21.35	21.13	32.10	34.67
Double layer capacitance, C_{cor} (F/cm^2)	8.97×10^{-9}	7.23×10^{-11}	5.48×10^{-11}	3.26×10^{-12}	1.70×10^{-8}	3.34×10^{-9}	1.77×10^{-6}
Corrosion resistance, R_{cor} ($\Omega.cm^2$)	6.29×10^{5}	4.38×10^{6}	7.37×10^{6}	3.34×10^{7}	7.45×10^{5}	4.20×10^{5}	1.66×10^{4}

Table 3: Circuit element values for scribed coatings after 60 hours

The scribed blank epoxy coating shows a relatively high double layer capacitance along with a relatively low corrosion resistance, and these values will be based on the normal passivation layer of aluminium found within the scribe region.

The addition of graphene to the epoxy appears to increase the corrosion resistance value from the epoxy blank, by up to two orders of magnitude for the 0.1 wt.% sample, and some increase in corrosion resistance is noted with a loading as low as 0.003 wt.%. The double layer capacitance is seen to decrease with the addition of graphene. This suggests that graphene is acting to increase the rate of passivation within the scribed region, and this is observed through the changes in corrosion resistance and double layer capacitance from the blank

epoxy sample. Impedance measurements have shown this material to have a greater impedance than the epoxy blank which suggests that graphene is acting both as a barrier and also to increase the rate of passivation at the scribe region.

The additional of RGO to the epoxy appears to make no real difference to both the corrosion resistance and double layer capacitance – both of these values are roughly similar to those obtained for the blank epoxy sample, regardless of loading, which suggests that RGO has no real impact on the rate of passivation of the aluminium. However, early impedance measurements and the salt spray testing suggest that RGO is acting more as a barrier type material, likely due to its lower electrical conductivity.

3.3 Potentiodynamic polarisation scans

Potentiodynamic polarisation scans permit considerable amounts of information on electrode processes to be determined. Through this technique, information on corrosion rate, pitting susceptibility, passivity and anode/cathode behavior of an electrochemical system may be obtained. During such scans, the driving force of the anodic/cathodic reactions (potential) is varied and the net change in reaction rate (the current) is measured. Tafel plots are usually displayed with the applied potential on the y axis and the logarithm of the measured current on the x axis, where the top half above the corrosion potential represents the anodic portion of the plot and the bottom half below the corrosion potential represents the cathodic portion of the plot.

Potentiodynamic scan experiments were conducted on an unscribed coating of 0.03 wt.% graphene in epoxy. In this case, with no direct access to the metal surface, the potentiodynamic scan shows no passivation occurring and relatively a high Tafel constant (indicating a low anodic reaction). This result is what we would expect to see from a coated sample where the coating itself acts as a barrier, and no passivation occurs (Figure 8)

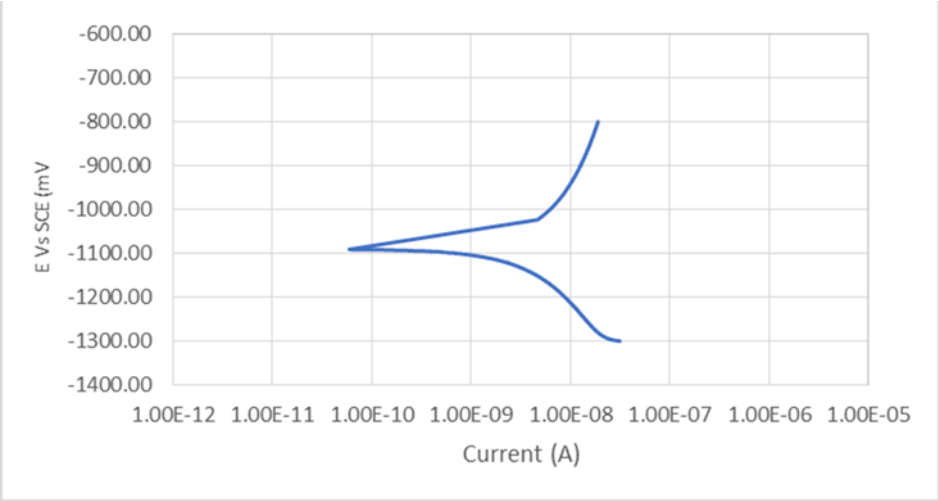

Fig.8: Potentiodynamic scan of an unscribed coating of 0.03 wt. graphene in epoxy

Adding a scribe to the coating allows direct access of the electrolyte to the metal surface (without waiting for the coating to degrade), and also allows graphene within the coating to contact with the metal surface. Potentiodynamic experiments were conducted on a scribed

coating of 0.03 wt.% graphene in epoxy resin. In looking at the potentiodynamic scan of this sample (Figure 9) the onset of passivation is observed at ~+18 mV from the corrosion potential for the scribed graphene-containing epoxy coatings, and this is not observed for the scribed samples containing no GNPs during the same timescale. A relatively a low Tafel constant is observed over the Tafel region, indicating a high anodic reaction.

Neither is the onset of passivation observed for the GNP-containing coatings with no scribe, where the coating itself acts as a barrier and no passivation occurs. The data suggests that the graphene is acting to increase the rate of passivation of the metal surface, acting in a catalytic manner to increase the rate of oxidation of aluminium to alumina within the scribed region. The increased passivation layer build up within the scribed region essentially acts to seal up the scribe in a self-healing type behaviour.

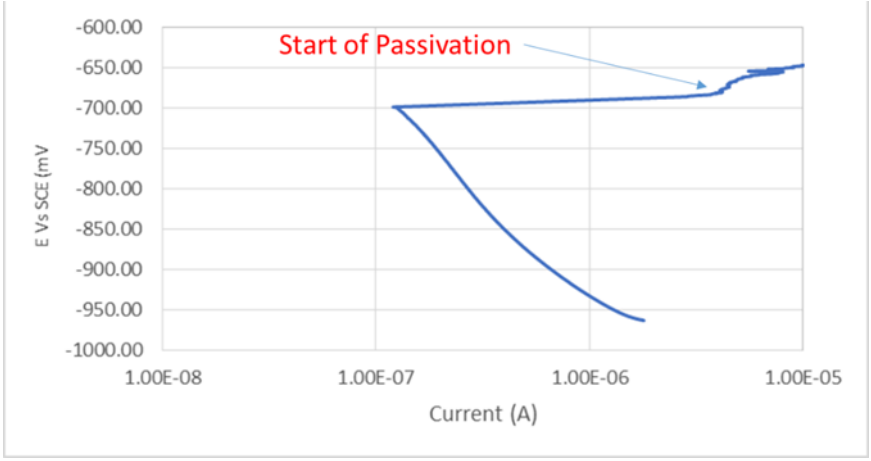

Fig.9: Potentiodynamic scan of a scribed coating of 0.03 wt. graphene in epoxy resin

If we then consider costings with a relatively lower electrical conductivity, based on RGO, we observe almost identical potentiodynamic plots for both the scribed and unscribed samples, and no passivation occurs in either of the samples. There is also little difference in the corrosion currents for both samples, which suggests that RGO is performing as a physical barrier, rather than controlling corrosion by accelerated passivation (Figure 10).

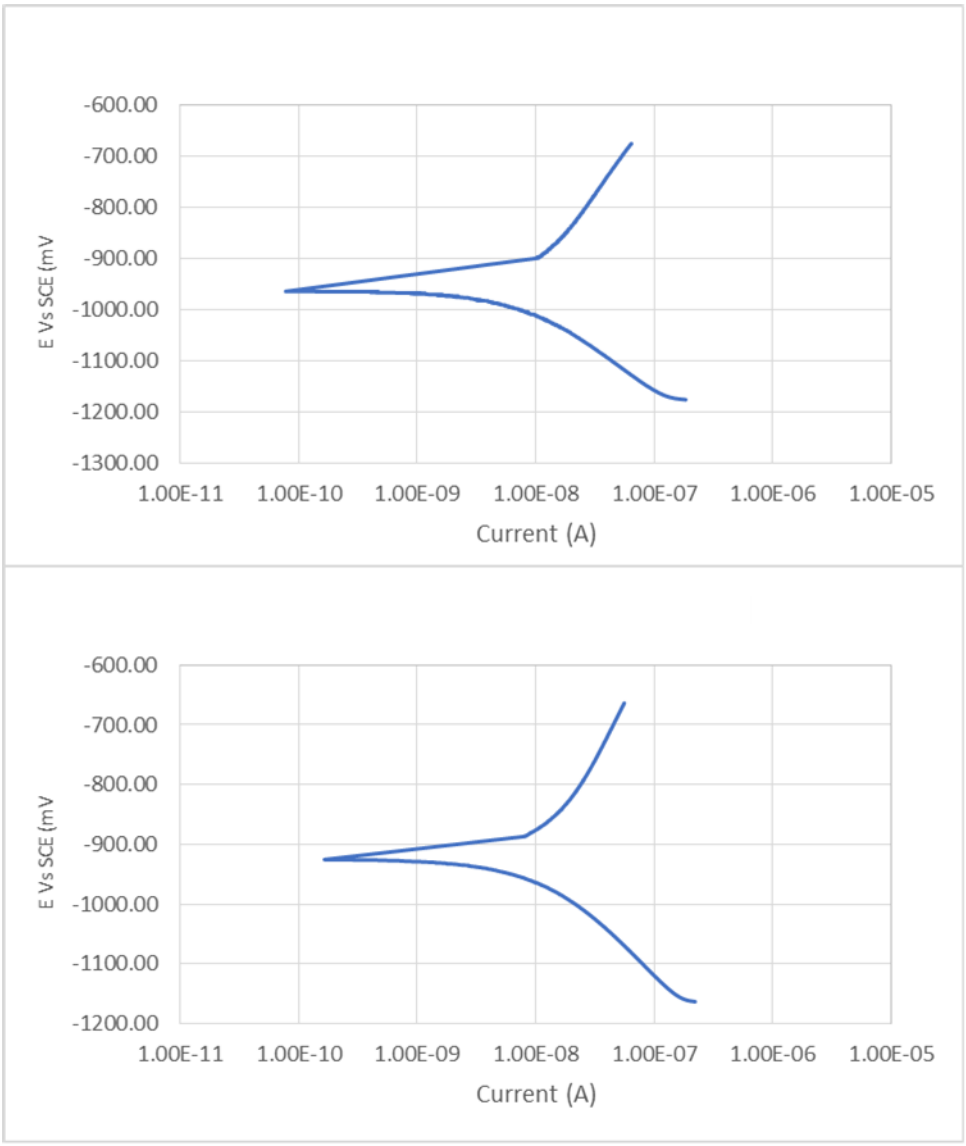

Fig. 10: Potentiodynamic scans of scribed and unscribed coatings of 0.03 wt. RGO in epoxy resin

Conclusions

Of the two different types of graphene material studied, graphene, of crumpled sheet like morphology and of 5-15 atomic layers, possesses a relatively high electrical conductivity. In contrast, RGO is composed of a mixture of more planar sheets, is of a higher oxygen content, and is of a comparably lower electrical conductivity than graphene.

Post 4000 hours of prohesion testing of coated panels, all graphene incorporated coatings (graphene and RGO) performed significantly better than the epoxy blank control sample, presumably either due to an enhanced physical barrier property of the coatings, and electrochemical influence from the graphene or a possible combination of both.

EIS measurements carried out over a relatively short term have shown that graphene incorporated at 0.1 wt.% into an epoxy provides a greater impedance than the blank epoxy control by an order of magnitude, while RGO incorporated at 0.5 wt.% shows an impedance value equivalent to the blank epoxy. Longer duration impedance experiments would be required in order to demonstrate the maintenance of these impedance values over time when graphene is incorporated into the coatings.

Equivalent circuit modeling of the impedance data, examining the interfacial circuit elements of scribed samples, has shown a progressive increase in corrosion resistance and a decrease in double layer capacitance for the more conductive graphene coated samples, where the epoxy blank and RGO samples have remained lower and fairly constant throughout. This suggests that graphene is acting to increase the rate of metal passivation within the scribed region. The relatively high impedance measurements of graphene suggests that graphene is acting both as a barrier and also to increase the rate of passivation at the scribe region. The fact that RGO appears to make little difference to corrosion resistance and double layer capacitance hints towards RGO providing a majority barrier type effect. Impedance values were found to be level with the epoxy blank in the short term, with the salt spray testing providing an indication that this impedance level is mentioned in the RGO samples where the epoxy blank drops off towards the poor protection region.

Additional electrochemical experimentation in the form of potentiodynamic polarisation scans has revealed the presence of an onset of passivation in the scribed graphene samples, where no such region can be found within the scans for the RGO incorporated samples or the epoxy blank. This again suggests the graphene is acting to increase the rate of passivation of the metal surface, acting in a catalytic manner to increase the rate of oxidation of aluminium to aluminum oxide, and the degree of passivation is dependent on the degree of conductivity exhibited by the GNP.

References

[1] R. Ding et al: Journal of Alloys and Compounds Vol. 764 (2018), p. 1039-1055

[2] K. Choi et al: ACS Nano Vol. 9 (2015), p. 5818 – 5824

[3] S. Aneja et al: FlatChem Vo1. 1 (2017), p. 11-19

[4] J. Crank and G. S. Park: Diffusion in Polymers, Academic Press, New York, NY, (1954)

[5] D. M. Brasher and A.H. Kingsbury: J. Appl. Chem, (1954), p. 62

[6] B. A. Boukamp, A. Rolle: Solid State Ionics Vol. 314 (2018), p.103-111

[7] A. Grammatikos et al: Composites Part A: Applied Science and Manufacturing Vol. 105 (2018), p. 108-117

[8] M. O'Donoghue et al: JPCL-PMC (1998), p. 36-51

[9] A. Hussain et al: Engineering Failure Analysis Vol. 82 (2017), p. 765-775

[10] G. Bouvet et al: Progress in Organic Coatings Vol. 77 (2014), p. 2045-2053

[11] T. Monetta et al: J. Coat. Technol. Res. (2018), p. 56-65